Electrochemical and Solid-State Letters, **15** (4) H133-H135 (2012)
1099-0062/2012/15(4)/H133/3/$28.00 © The Electrochemical Society

Thermal Evolution of Band Edge States in ZnO Film as a Function of Annealing Ambient Atmosphere

Hyun-woo Park,[a] Jin-Seong Park,[b] Ju Ho Lee,[c] and Kwun-Bum Chung[a,z]

[a]*Department of Physics and* [b]*Department of Materials Science and Engineering, Dankook University, Cheonan 330-714, Korea*
[c]*Department of Materials Science and Engineering, Korea Advanced Institute of Science and Technology, Daejeon 305-701, Korea*

RF-sputtered ZnO films were annealed under various annealing ambient atmospheres, including a vacuum, air, and water vapor. The physical and electrical properties of ZnO films annealed in various ambient atmospheres, were studied as a function of annealing temperature. The carrier concentration was dramatically increased, and the mobility was decreased when the films were annealed in a vacuum or water vapor. Even though the annealing ambient atmosphere and temperature were different, the preferred orientation and crystallization of the annealed ZnO films are maintained. However, two distinct band edge states below the conduction band, observed by spectroscopic ellipsometry measurement, undergo a thermal change as a function of annealing ambient atmosphere and these changes are correlated to changes in carrier concentration and mobility.
 [DOI: 10.1149/2.005205esl]

Manuscript submitted October 13, 2011; revised manuscript received January 16, 2012. Published February 7, 2012.

N-type ZnO material with wide-bandgap (~3.3 eV) has been investigated for a wide range of applications, such as UV light emitters, spintronic devices, transparent high-power electronics, surface acoustic wave devices, piezoelectronic transducers, gas and biological sensors, and solar cells.[1,2] In particular, ZnO-based thin film transistors (TFTs) are very attractive in flexible and transparent electronics because the devices show the moderate hall mobility (>1 cm^2/V.s) even on room temperature and the ZnO semiconductors is transparent in the visible range.[3]

Recently, several researchers have reported TFTs application using stoichiometry ZnO semiconductor by various deposition methods.[4,5] However, the devices usually showed high off-current (>10^{-11}A) and poor on/off ratio of drain current, which is very important factor to decide switching modulation of devices, since the resistivity of ZnO film is very sensitive on oxygen states during the deposition or post-treatment. Thus, the major interest of these researches is the modulation of ZnO material properties, such as carrier concentration and mobility with simple processing conditions. The modification of ZnO properties were achieved by impurities doping, ion implantation, annealing process and the other method.[6] Unfortunately, the impurities doping into ZnO films have induced in high cost and complication for doping elements. The ion implantation also produces the collision damage into ZnO matrix, which can generate unnecessary and uncontrollable defect states.[7]

In this study, we examine the effects of simple thermal treatments under various annealing ambient atmospheres on ZnO films, in terms of physical, and electrical properties. Moreover, physical origins of change in electrical properties of ZnO films are investigated and are analyzed by the evolution of band edge states as a function of thermally driven energy.

Experimental

P-type Si wafers with thermally grown SiO_2 (100 nm) were used as substrates onto which ZnO films (50 nm) were deposited without the substrate heating by a radio frequency (RF) sputtering system. The RF power and process pressure were set to 75 W and 10 mTorr, respectively, which was controlled by an Ar gas flow rate of 50 sccm. After that, ZnO films were annealed by a furnace system with a quartz tube and quartz loading bar. The annealing duration was 1 hour and the temperature was at 150°C, and 300°C. In order to examine the effects of the post-annealing, the annealing ambient atmosphere was maintained for air, vacuum, and water vapor conditions. The annealing in the ambient atmosphere of air was performed on the day had humidity of ~38% The vacuum ambient atmosphere was controlled by a rotary pump to maintain a pressure below 5×10^{-2} Torr. The water vapor ambient atmosphere was produced using a water bubbler system with a N_2 gas flow of 100 sccm. Water vapor annealing was carried out at 10mtorr using a rotary pump and throat valve. In order to the electrical properties such as carrier concentration and hall mobility of ZnO films, Hall measurements were carried out using van der Pauw configuration with the permanent magnet of 0.55 Tesla at room temperature. The crystallization and its orientation of the annealed ZnO films were observed by transmission electron microscopy (TEM),and X-ray diffraction (XRD). The surface morphology was investigated by using atomic force microscopy (AFM). The detailed electronic structures, related to changes in bandgap and band edge state below the conduction band, were analyzed by spectroscopic ellipsometry (SE).

Results and Discussion

Figure 1 shows the electrical properties, including the carrier concentration and mobility of the ZnO films as a function of annealing ambient atmosphere and temperature. In as-deposited ZnO film, the carrier concentration and mobility were 1.2×10^{14} cm^{-3} and 107 $cm^2V^{-1}s^{-1}$, respectively, and the films displayed *n*-type semiconductor characteristic. When the annealing temperature was increased to 150°C, the carrier concentration shows small variations under the value of ~10^{15} cm^{-3} and the mobility represents the similar value, regardless of annealing ambient atmosphere. However, at the annealing temperatures over 300°C, the carrier concentration was dramatically increased to ~10^{19} cm^{-3} and the mobility was decreased to ~10 $cm^2V^{-1}s^{-1}$ in the ambient atmosphere of a vacuum and water vapor, which is reasonable value comparing to the previous report.[8] These remarkable changes in carrier concentration and mobility could be associated with the carrier generation and the increase of electron scattering by the evolution of defect states such as oxygen vacancies, which are affected by the annealing ambient atmosphere.[9] More discussion is provided below and considers the physical and electronic structure.

Figure 2a shows the selected area diffraction (SAD) patterns of the ZnO films annealed in an ambient atmosphere of air as a function of annealing temperature. The SAD images represent the ring patterns, which mean that the ZnO film is the nano-crystalline structure before and after annealing. Also, these nano-crystalline structure have the preferred z-axis orientation of a hexagonal ZnO (0002) by confirmation of XRD spectra (not shown in here). The thermal evolution of physical structure indicates that different annealing ambient atmosphere and temperature below 300°C have no changes of

[z] E-mail: kbchung@dankook.ac.kr

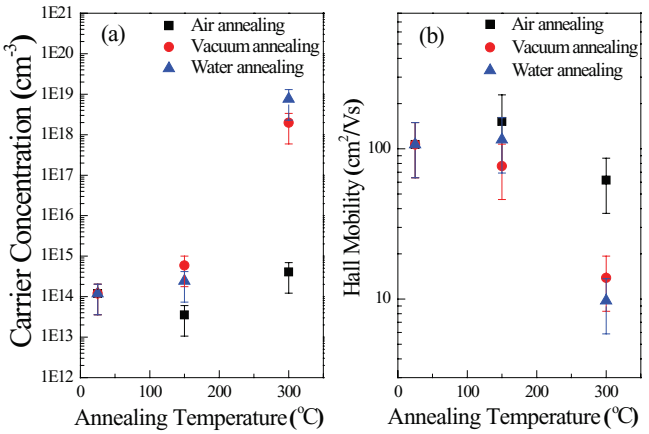

Figure 1. (a) Carrier concentration and (b) Hall mobility of the as-deposited and annealed ZnO films as a function of annealing ambient atmosphere.

physical crystalline structure. In order to investigate the surface morphology, the plane view of TEM and AFM images were obtained as shown in Figure 2b. The surface morphology shows the similar image, of which grain size and rms surface roughness are preserved with ~140 nm^2 and 0.5 ~ 0.7 nm, respectively. Therefore, the changes of nano-crystalline structure, grain size and surface morphology were severely not observed after annealing, regardless of annealing ambient atmospheres.

In order to investigate the electronic structure of the films, including the band edge states below the conduction band, SE data were taken as a function of annealing ambient atmosphere and temperature. The spectroscopic ellipsometry (SE) is a nondestructive technique to measure the optical response and absorption of materials. Recently, the interpretation for the unoccupied states in conduction band and sub-band states by SE analysis has been paid an attention. Our previous report showed the correlation between the oxygen vacancies and the band edge states below the conduction band by SE measurement for HfO_2 on Ge.[10] Even if as-grown un-doped ZnO always show *n*-type conductivity, but the origin of the *n*-type conductivity is still controversial. Some research has reported that the hydrogen impurities, zinc antisites, and oxygen vacancies are a origin of electrical properties of ZnO.[11,12] However, we will discuss the change of electrical properties of ZnO films as a function of native defects such as oxygen vacancy, based on the experimental absorption states observed by SE. The imaginary dielectric function (ε_2) spectra for the as-deposited ZnO films on Si substrates are shown in Figure 3a. These spectra were extracted from a simple four-phase model, which

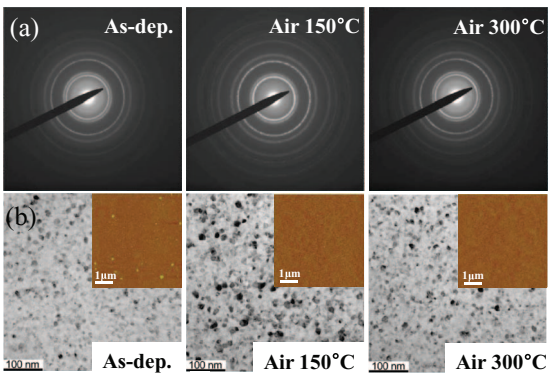

Figure 2. (a) SAD patterns of TEM and (b) the plane view images of TEM and AFM images from the as-deposited and annealed ZnO films in an ambient atmosphere of an air as a function of temperature.

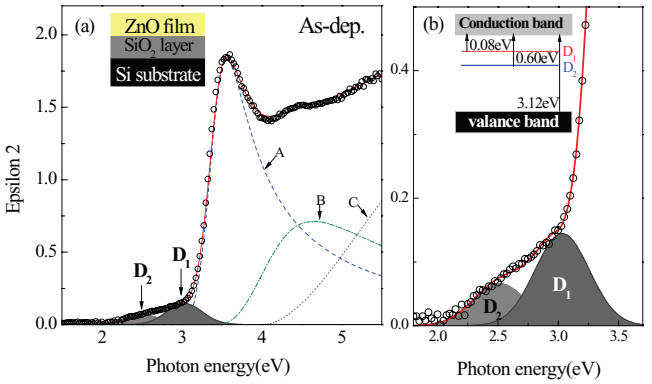

Figure 3. (a) Imaginary dielectric function (ε_2) spectra from SE measurements for the as-deposited ZnO film. The deconvoluted peaks, labeled A, B, and C are model fits using Tauc-Lorentz function. Two distinct deconvoluted peaks, labeled D_1 and D_2 are Gaussian fits and represent the band edge states located below the conduction band edge. (b) Enlargement of the band edge states below the bandgap near ~3.1eV and an energy diagram above valence band. The diagram of the inset describes the energy levels of the band edge states (D_1 and D_2) below the conduction band edge.

is comprised of a Si substrate, SiO_2 overlayer, ZnO overlayer, and an ambient layer as shown in the inset of Figure 3a.[13] The solid line in Figure 3a is obtained from the sum of deconvoluted functions, A, B and C. The best fit parameters are listed in Table I. The physical meaning of respective function is the contribution by the various types of transitions; A for the one-electron contribution, B for the discrete-exciton contribution, and C for the continuum-exciton contribution.[14] The features that can be seen at the onset energy above the optical bandgap around ~3.1 eV indicate the unoccupied states of the ZnO, which correspond to the hybridized molecular orbital states mixed by the Zn 4*sp* and O 2*p* states.[15,16] A detailed and quantitative analysis of the band edge states and unoccupied states in the conduction band was performed by fitting using a Gaussian model (band edge states) and a Tauc-Lorentz model (conduction band states). The Gaussian fit function is $\varepsilon_{2_{Gaus}} = Ae^{-\left(\frac{E-E_n}{\sigma}\right)^2} - Ae^{-\left(\frac{E-E_n}{\sigma}\right)^2}$, $\sigma = \frac{B_r}{2\sqrt{\ln(2)}}$, where A, E_n, and B_r denote the amplitude, peak transition energy, and broadening parameter, respectively. The Tauc-Lorentz model fit is obtained by the following imaginary dielectric function;

$$\varepsilon_{2_{TL}}(E) = \left[\frac{AE_nC(E-E_g)^2}{(E^2-E_n^2)^2+C^2E^2}\cdot\frac{1}{E}\right], \quad E > E_g$$
$$= 0, \quad E \le E_g$$

where the subscript TL indicates that the model is based on the Tauc joint density of states and the Lorentz oscillator.[17] The four fitting parameters E_g, A, E_n, and C denote the bandgap energy, the amplitude, peak transition energy, and broadening parameter, respectively. The fitting curves of the as-deposited ZnO films are included in Figure 3a and the fitting parameters are summarized in Table I. The

Table I. Gaussian fitting parameters of the band edge states (D_1 and D_2) and Tauc-Lorentz model fitting parameters of the conduction band states for the as-deposited ZnO film.

		Gaussian model			Tauc-Lorentz model		
	Parameter	D_1	D_2	Parameter	A	B	C
As-dep	*Amp*	0.07	0.14	*Amp*	51.33	30.20	81.00
	$E_n(eV)$	2.51	3.03	$E_n(eV)$	3.42	4.04	5.92
	$B_r(eV)$	0.52	0.53	$C(eV)$	0.59	1.59	7.51
				$E_g(eV)$	2.98	3.46	4.00

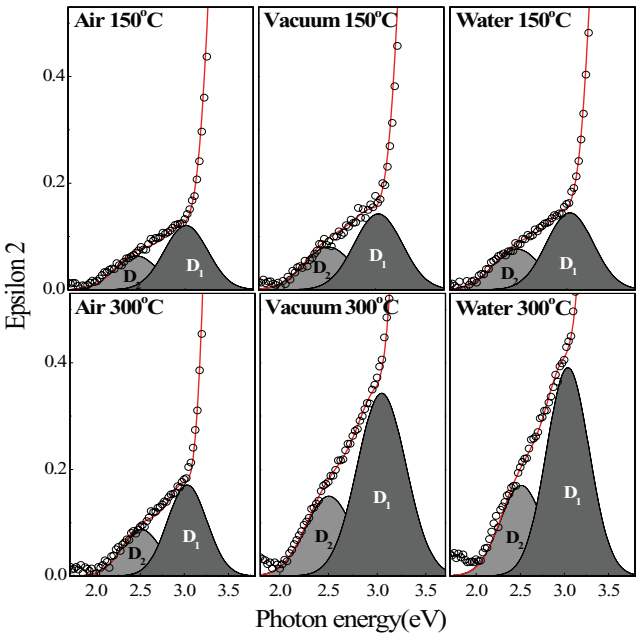

Figure 4. Thermal evolution of the band edge states over a narrow energy region below the conduction band edge as a function of annealing ambient atmosphere. The energies of D_1 and D_2 are the center energies for D_1 and D_2 Gaussian fits from the conduction band edge (3.12 eV). The determination of the center energies for D_1 and D_2 Gaussian fits is accomplished from the analysis of second-derivative of original spectrum.

Gaussian model fits are comprised of two distinct band edge states with a shallow band edge state (D_1) and deep band edge state (D_2), which are located at 0.08 eV and 0.60 eV away from the conduction band edge, respectively. Figure 3b represents an enlargement of the band edge states below the conduction band edge near ~3.1 eV and an energy diagram of the above valence band. The diagram describes the energy level of the band edge states (D_1 and D_2) below the conduction band edge.

Figure 4 shows the thermal evolution of the band edge states below the conduction band as a function of annealing ambient atmosphere. The annealed ZnO films in air ambient atmosphere show slight changes in the band edge states with increasing annealing temperature. On the other hand, the annealed ZnO films in the ambient atmosphere of a vacuum or water vapor, induce the drastic increases in the band edge states for D_1 and D_2 after annealing at 300°C. Considering the previous electrical data, the variation of D_1 and D_2 states is strongly correlated with the increase of carrier concentration and the degradation of mobility. Based on the SE analysis, the most plausible origin of the changes in electrical properties such as carrier concentration and mobility could be attributed to the thermal evolution of the band edge states as a function of annealing ambient atmosphere, which is related to oxygen vacancies.[18] The increase of carrier concentration with annealing in an ambient atmosphere of a vacuum or water vapor, may be explained by the increase of the shallow band edge state (D_1) because it means that the number of free electron which can conduct as a carrier is getting lager by the generation of oxygen vacancy.[19] Another interesting interpretation for mobility is associated with the deep band edge state (D_2). Even if the shallow band edge state (D_1) is the possible origin to enhance the charge transport through the unoccupied states caused by oxygen vacancy, the deep band edge state (D_2) can have higher effect on the degradation of mobility because of the charge trapping and the increase in charge scattering during carrier transport due to energy levels far from the conduction band.[20] From the above interpretations, the changes in the band edge states, induced by oxygen vacancies, contribute to the modification of the carrier concentration and mobility in annealed ZnO films as a function of annealing ambient atmosphere.

Conclusions

RF-sputtered ZnO films were annealed in various annealing ambient atmosphere, including air, a vacuum, and water vapor. The annealing in the ambient atmosphere of air results in only small changes of carrier concentration and mobility regardless of the annealing temperature. However, in the annealing ambient atmosphere of a vacuum or water vapor, the carrier concentration is increased to $\sim 10^{19}$ cm^{-3} while mobility is degraded when the annealing temperature is increased up to 300°C. The structural transition and modification are preserved, with the crystalline oriented by the hexagonal ZnO (0002) phase, regardless of annealing ambient atmosphere and temperature, and have no connection with the electrical properties. On the other hand, the thermal evolution of the two distinct band edge states as a function of annealing ambient atmosphere, observed below the conduction band and interpreted as oxygen vacancies, are correlated to the changes in carrier concentration and mobility. The increase of carrier concentration in the annealing ambient atmosphere of a vacuum or water vapor could be related to the increase of the shallow band edge state, and the degradation of mobility could be associated with the increase of the deep band edge state.

Acknowledgments

This research was supported by Basic Science Research Program through the National Research Foundation of Korea (NRF) funded by the Ministry of Education, Science and Technology (2011-0004901).

References

1. A. Tsukazaki, A. Ohtomo, T. Onuma, M. Ohtani, T. Makino, M. Sumiya, K. Ohtani, S. F. Chichibu, S. Fuke, Y. Segawa, H. Ohno, H. Koinuma, and M. Kawasaki, *Nat. Mater.*, **4**, 42 (2005).
2. Myung-Gil Kim, Mercouri G. Kanatzidis, Antonio Facchetti, and Tobin J. Marks, *Nat. Mater.*, **10**, 382 (2011).
3. E. M. C. Fortunato, P. M. C. Barquinha, A. C. M. B. G. Pimentel, A. M. F. Goncalves, A. J. S. Marques, L. M. N. Pereira, and R. F. P. Martins, *Adv. Mater.*, **17**, 590 (2005).
4. S.-H. Park, C.-S. Hwang, M. Ryu, S. Yang, C. Byun, J. Shin, J.-I. Lee, K. Lee, M. S. Oh, and S. Im, *Adv. Mater.*, **21**, 678 (2009).
5. P. F. Carcia, R. S. McLean, M. H. Reilly, and G. Nunes, Jr., *Appl. Phys. Lett.*, **82**, 1117 (2003).
6. Shigemi Kohiki, Mikihiko Nishitani, Takahiro Wada, and Takashi Hirao, *Appl. Phys. Lett.*, **64**, 2876 (1994).
7. M. Schmidt, M. Ellguth, and F. Schmidt, *Phys. Status Solidi B*, **247**, 1220 (2010).
8. Ü. Özgür, Ya. I. Alivov, C. Liu, A. Teke, M. A. Reshchikov, S. Doğan, V. Avrutin, S.-J. Cho, and H. Morkoç, *J. Appl. Phys.*, **98**, 041301 (2005).
9. K. Jwayeon, K. Myung-chun, Y. Jaekeun, and P. Kyeongsoon, *Curr. Appl. Phys.*, **10**, S495 (2010).
10. K. B. Chung, H. Seo, J. P. Long, and G. Lucovsky, *Appl. Phys. Lett.*, **93**, 182903 (2008).
11. Anderson Janotti and Chris G. Van de Walle, *Phys. Rev. B*, **76**, 165202 (2007).
12. F. Oba, A. Togo, I. Tanaka, J. Paier, and G. Kresse, *Phys. Rev. B*, **77**, 245202 (2008).
13. D. E. Aspnes and A. A. Studna, *Phys. Rev. B*, **27**, 985 (1983).
14. Hisashi Yoshikawa and Sadao Adachi, *Jpn. J. Appl. Phys.*, **36**, 6237 (1997)
15. P. A. Cox, *Transition Metal Oxides* (Clarendon, Oxford, 1992).
16. Veeramuthu Vaithianathan and Byung-Teak Lee, *Appl. Phys. Lett.*, **88**, 112103 (2006).
17. G. E. Jellison, Jr. and F. A. Modine, *Appl. Phys. Lett.*, **69**, 371 (1996).
18. Hyungtak Seo, Chan-Jun Park, Young-Je Cho, Young-Bae Kim, and Duck-Kyun Choi, *Appl. Phys. Lett.*, **96**, 232101 (2010).
19. T. Kamiya, K. Nomura, and H. Hosono, *J. Disp. Tech.*, **5**, 273 (2009).
20. K. B. Chung, J. P. Long, H. Seo, G. Lucovsky, and D. Nordlund, *J. Appl. Phys.*, **106**, 074102 (2009).